International Conference on Space Optics—ICSO 2018

Chania, Greece

9–12 October 2018

Edited by Zoran Sodnik, Nikos Karafolas, and Bruno Cugny

Tailored dispersive elements for adapted spectrometric sensing

Torsten Diehl

Peter Triebel

Tobias Moeller

Alexandre Gatto

et al.

International Conference on Space Optics — ICSO 2018, edited by Zoran Sodnik, Nikos Karafolas, Bruno Cugny, Proc. of SPIE Vol. 11180, 111801K · © 2018 ESA and CNES · CCC code: 0277-786X/18/$18 · doi: 10.1117/12.2535975

Tailored dispersive elements for adapted spectrometric sensing

Torsten Diehl, Peter Triebel, Tobias Moeller, Carl Zeiss Spectroscopy GmbH (Germany);
Alexandre Gatto, Dennis Lehr, Alexander Pesch, Lars H. Erdmann, Matthias Burkhardt;
Alexander Kalies, Felix Koch, Carl Zeiss Jena GmbH (Germany)

ABSTRACT

Dispersive elements are in general the key components of spectrometers and define mainly their performance. Prisms and filters are typically used for lower resolution applications, e.g. color measurement for industrial applications. Many high performance spectrometer applications are using gratings as dispersive elements instead. Different spectrometer layouts require various grating approaches in order to maintain the optical imaging performance. A frequent aim is a progressively optimization of the optical performance in balance to the mechanical parameters like weight, volume or robustness against variations of environmental conditions of a spectrometer module as well. Thus, the optical designer has to draw on additional design degrees of freedom. This in turn results often in more and more complex grating types featuring curved substrates and/or variable and bended grating lines. Especially the trend toward hyperspectral imaging applications demands appropriate options for enhanced field correction. The main ZEISS technology chain for grating manufacturing includes holography and reactive ion etching is a flexible base for these special types of gratings. A close entanglement between holography and accurate test procedures for the optical functionality of the holographic grating is a pre-condition for the ability to meet the often challenging specifications. Therefore, beside the brief description of the manufacturing technology in this text we show a set of newly developed measuring procedures supporting the holographic surface patterning approach.

Keywords: diffractive optics, grating, custom design grating, aberration-corrected grating, free-form or toroidal grating, monolithic grism, holography, interference grating, ion etching, remote sensing application

1. GRATING MANUFACTURING USING MODERN MICRO STRUCTURING TECHNOLOGIES

Numerous processes can be used for grating manufacturing with different characteristics and grating profiles. Common processes for optical gratings are e-beam lithography [1], ruling, Direct-Laser-Writing (DWL) and holography. According to our experience holography or interference lithography is the best choice to generate almost arbitrary coherent grating structures on a manifold of substrate types. Further, on any substrate shape gratings with high peak efficiencies due to the option for blazing and least levels of ghost and stray light are feasible [5].

Holography is a parallel grating generation process that allows the pattern generation simultaneously on the entire optical surface [2-5]. As indicated in Fig. 1 a substrate may be curved as well. The handling of comparable heavy and/or very extended or thick or non-planar prism-like substrates is possible because there is in general no need to move the blank during the recording process. This is in contrast to the majority of the serial writing techniques. The common holographic approach is shown in Fig. 1, left side. This setup version generates generally sinusoidal symmetric grating profiles in the photoresist [6]. Especially if the depth of development is moderate – as indicated for example by the blue dotted curve in Fig. 3 left side – the resulting profile is close to an ideal sinus-shape. An optional subsequent ion etching process can be employed to transform these profiles into a blaze profile too. This approach has some drawbacks depending on the employed etching machine. In general, the angle of resulting blaze facets is globally oriented in the same direction. This leads to a more or less disturbing local variation of the grating efficiency. The situation gets worse if the surface angle variation of a curved substrate exceeds the magnitude of the blaze angle – as typical for EUV-gratings due to the comparable shallow blaze profiles.

For the generation of blaze profiles directly in the resist Fig. 1. right side shows the adequate setup. This holographic approach is using counter-propagating waves in relation to the substrate surface. The geometries lead to the generation of a tilted stack of interference layers during the recording step. The final wet chemical

development unveils a well approximated blazed profile [9, 10]. Distinguishing mark of these technique is a locally adapted blaze angle supporting the diffraction into a desired order in an optimal way [11].
The holographic principles, the resulting interference pattern and the typical photoresist profiles are shown in Fig. 1, Fig. 2, Fig. 3 and Fig. 4.

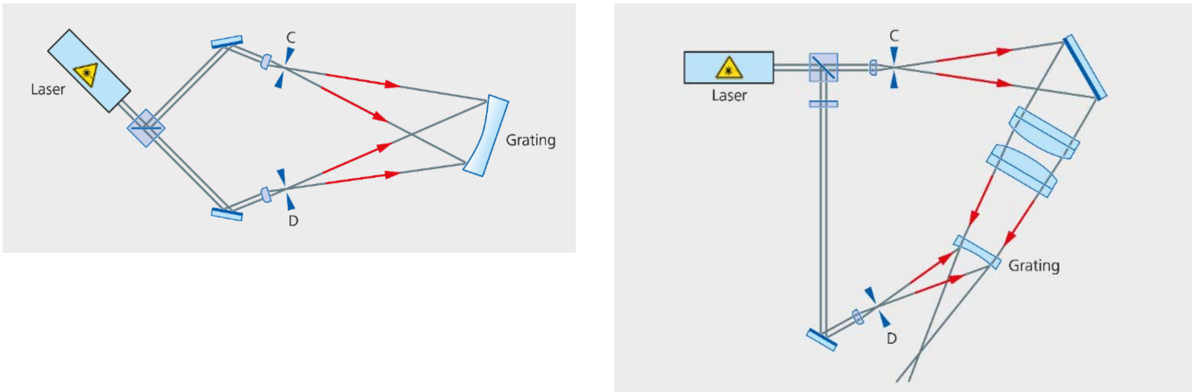

Fig. 1: The principle holographic setup approaches are shown. Left side: the symmetric holographic exposure setup, right side: in relation to the substrate surface the waves are primarily counter propagating

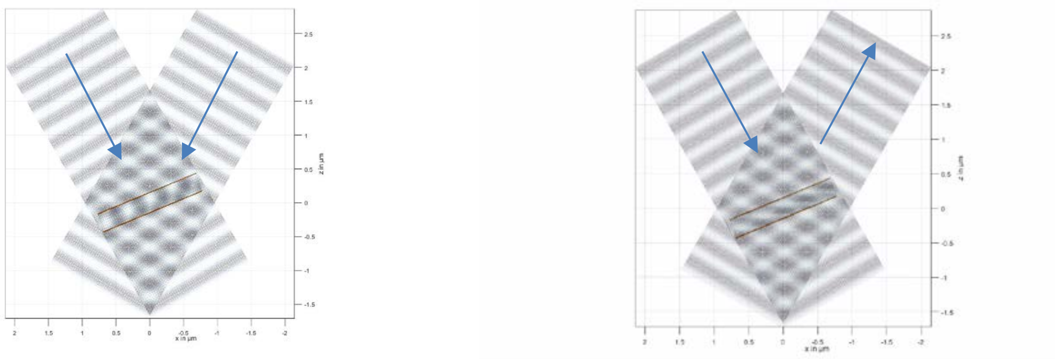

Fig. 2: Left side: the interference pattern resulting from a symmetric holographic exposure setup, right side: interference pattern resulting from the opposing wave approach

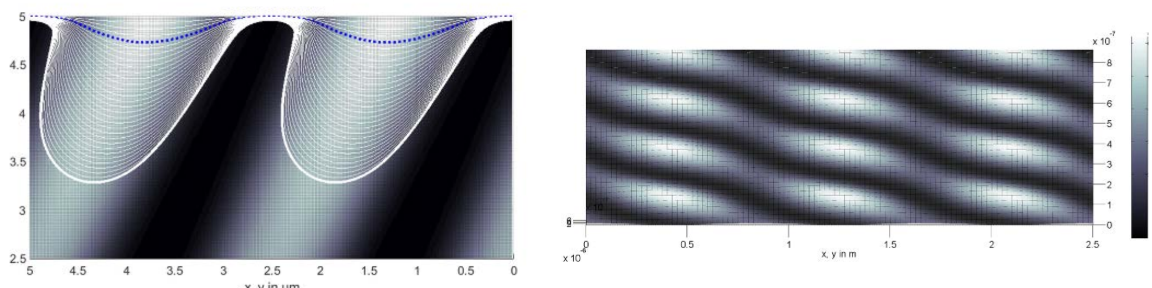

Fig. 3: Left side: photoresist grating simulation with a nearly symmetric profile due to holographic exposure setup in Fig. 1 left, right side: typical spatial modulation of solubility for counter propagating waves

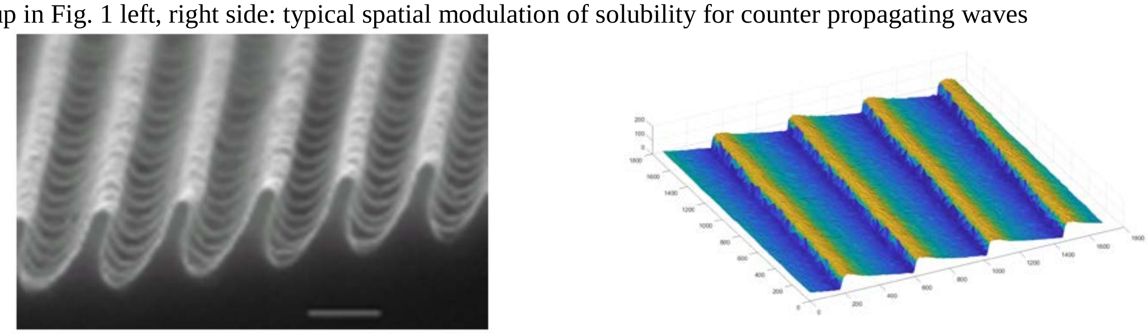

Fig. 4: Left side: deep developed photoresist grating SEM picture with a nearly symmetric profile (tilted symmetric exposure), right side: photoresist grating AFM picture (opposing wave approach)

2. OPTIMIZATION INCLUDING CUSTOM SPECIFIC DEMANDS AND MANUFACTURING TECHNOLOGY

In a spectrometer systems optimization step it is beneficial if the optical designer doesn't have to regard the current constraints of serial writing or ruling processes for the manufacturing of diffraction gratings. In this context holography provides a technological base for classical grating types like Offner- or Rowland-type gratings – even if the desired radii of curvature are comparable small. In general a variation of surface angles exceeding ±10 degrees within the clear aperture are manageable by holography as well. Further, concave imaging gratings or gratings defined by a variable line spaces definition (VLS gratings) are feasible. In general a close cooperation between grating manufacturer and the manufacturer of the spectrometer in early project states helps to find out the optimal grating type with regard to the systems performance as well as to a save technological path for the grating.

Proceeding from classical grating types, additional optical design parameters with various degrees of freedom can be used for the implementation of aberration corrected gratings and VLS (variable line space) gratings. Both types of gratings are highly appropriate for holographic exposure. Commonly a recording setup can be derived from any customers grating description based on substrate surface figure and line density distribution. Optional optimization loops incorporating all of the spectrometers optics may often lead to extra well adapted holography setups. This kind of a global optimization works with fixed parameters for the elements of the spectrometer. Further, proceeding with the initial merit function the line density distribution will be still close to the classical grating description. Additionally, the potential for bending the lines and/or use higher order coefficients in case of a VLS grating can be employed for achieving enhanced focusing properties or imaging quality.

Beside the optimization of the imaging performance, the parameters efficiency and polarization sensitivity will influence the system performance of spectral remote sensing systems [7]. The manufacturing method of the grating also predefines the type of the grating profile. Therefore the recording type has to be set regarding the desired spectral energy efficiency. All mentioned grating types above are available with symmetrical grating structures or with blazed profiles depending on what is the best choice for the application. A tuning of the spectral efficiency curve can be achieved by scaling the initial profiles in the height dimension.
The often preferred initial (resist-) blazed profile lead in most cases to more complex recording setups including expensive special optical parts. During a conception phase ray tracing based simulations are used to simulate and optimize the holographic recording setup with its individual optical elements including the calculation of tolerances. The design of the exposure optics is adapted to achieve highest imaging quality with respect to blaze profile, correct grating line orientation and groove density variation. Beside this optimization, based on the customer's spectrometer design an angular range of interest (field of view) can be defined in order to optimize the holographic setup towards unwanted back-reflections or false light, which can lead to unwanted satellites with minor intensity [7]. In most cases, the optimization of the holographic setup can be realized by using special designed optical elements for compensation of aberrations while avoiding these unwanted back-reflections. In order to secure the optical performance of this often preferred blaze profile even on complex grating types an adapted inspection technique has to be provided.

3. WAVEFRONT MEASUREMENT RESULTS OF AN ABERRATION CORRECTED GRATING

Plane and curved gratings with moderate curvature and tiny deviations from an equidistant line distribution can be tested by a conventional interferometer. The typical interferometer measurement for optical surfaces employs the 0th order of a sample. To assess the optical performance of a grating or a holographic element one of the accessible higher diffraction orders is captured. This approach is limited to wave front curvatures that lead to line densities below the Nyquist-frequency of the measuring system – mainly limited by the pixel sizes of the detector array. Thus, in practice many grating types - including concave imaging gratings, Offner-gratings or aberration corrected and VLS-gratings - are not measurable by this method. Therefore we use adapted strategies to ensure the quality of the huge variability of diffractive elements manufactured by our in house technology.

a) Test of non-imaging classical grating types (e.g. Offner, Rowland type gratings)

Prior to the grating pattern evaluation, an interferometric measurement of the substrate provides the information of the optical quality referring to the surface figure.

A valid favored model for the description of the observed intensity distributions during the measurement is based on the Moiré-principle. This model is absolutely equivalent to the outcome if the laws of diffraction and interference are applied. A close relationship to holographic interferometry exists as well. However, the Moiré-principle is thought as a far more easy-of-access approach. The first example addresses the accurate inspection of the line density distribution of a convex grating for an Offner-system. Its surface angles vary by ±9 degrees. Here one can get a benefit from the fact that an equidistant and parallel line distribution is given if the grating lines are projected onto a tangential plane through the vertex of the grating substrate. This means that a comparison between the convex grating and a virtual plane grating – extended along the optical axis of the convex Offner-grating substrate – may provide a suitable procedure. Thus we use a periodic standing wave pattern – the interference field - generated by two coherent plane waves as reference for the evaluation of the sample. By employing in house manufactured high quality optics we achieve a wave front error less than lambda/20 in every slice of the interference pattern. Now let's regard the interference field as an incorporation of an extended grating structure. After a symmetrical alignment of the grating sample as well as an adaption of the interference field to the projected line density a mismatch between the lines of the convex grating and the periodical spatial intensity modulation results in a characteristic Moiré-pattern.

In Fig. 5 one can see a typical image on a screen that was captured by a camera. Here the clear aperture of the grating is of circular shape. To simplify the analysis the corners of the surrounding square matrix in Fig. 5 right are filled with the grey levels of the circle border-pixels in each pixel column. This approach avoids any unambiguity for the analysis. Note that the periodic part of the Moiré-fringe pattern is intended with regard to the simplification of the numerical processing too. This part corresponds to a slight tilt and can be removed easily to plot only the wave distortion.
Using this kind of line patterns a camera image of a projection screen that is arranged in a direction where the ±1st diffraction orders interfere is sufficient to get the necessary information about the absolute value of the wave distortion (Fig. 6). Another image with only a slight phase shift in one of the interfering plane waves for the test field allows the determination of the sign of deformation as well. The mentioned overlap of the ± 1st diffraction orders indicates that in this example the frequency of the interference field is two times as high as the grating line density. Under these conditions the method works still fine but then one period in the Moiré-pattern corresponds to a relative mismatch of only a half of the grating period. When employing conventional interferometer software the wave distortion function has to be divided by 2.

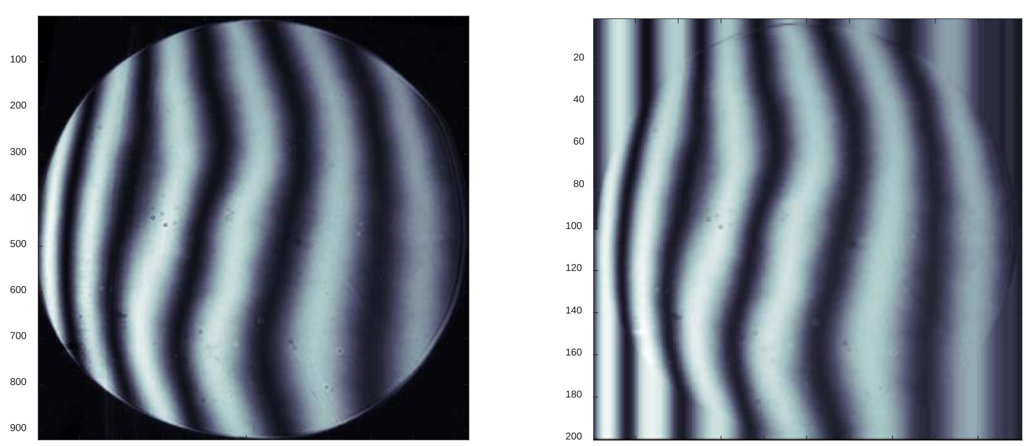

Fig. 5: left side: a typical Moiré-pattern generated by a test setup for an Offner-grating in an even interference field, right side: extended pattern to achieve a square matrix that is beneficial for the numerical processing – the numbers on the x- and y- axes indicate pixel numbers

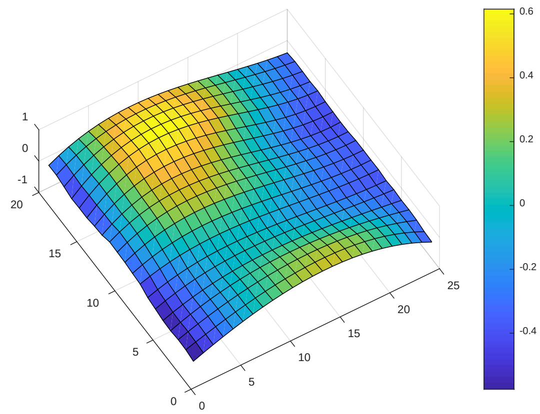

Fig. 6: Moiré lines transferred into a surface figure of a corresponding wave front, by this method an optical designer is able to predict the performance of a spectrometer system – the information about the wave aberration is coded in the distance and curvature of the fringes – the examples shows a PV-value for the wave aberration of about 0.8 periods (note the edges have to be neglected)

b) VLS gratings with no imaging function under test conditions

More challenging test objects are gratings with or without curvature and with a comparable strong variation of the line density along the grating vector. Though it is in some cases a possible way to include a CGH in the optical path of an interferometer VLS as well as aberration corrected gratings in general offer another more flexible way to test them accurately. Here we show an example based on a precisely aligned static interference field (according to the Offner-grating measuring setup described above) combined with a VLS grating sample. Fig. 7 a) shows the Moiré-pattern for this blazed VLS grating on a toroidal substrate embedded in the projected clear aperture. The grating design exhibits a symmetrical line distribution in grating line direction at its vertex. It was manufactured with a holographic recording process and due to the additionally holographic aberration correction, the sample has neither equidistant nor straight grating lines. Therefore an even periodic test field leads only to a locally constrained phase match area indicated by the elliptical zero-interference region (zero-Moiré-region) close to the center of the figure.

The initial alignment of the interference field is careful carried out by using a reference grating. The spatial frequency of the interference field has to be at least as high as the highest line density on the grating surface. After this alignment procedure one will observe at least a small grating region that fits to the spatial frequency of the test field as indicated by the examples in Fig. 7. Then a defined change of the period of the interference field relative to the sample surface generates a local shift of the best matching area. A rotation axis perpendicular to the grating vector in the vertex leads to a lateral shift along the dispersion direction of the grating. The local matching between interference field and grating frequency can be modified preferably by a defined rotation of the grating (Fig. 7 c) or a rotation of a plane wave in the interference field or of both waves. If the rotation continues the best matching area will migrate further until a set of sampling points - sufficient for a retrieval of the line density distribution - is gathered. Detecting the location of this zero-interference-region precisely and associate it to the corresponding rotation angle an accurate assignment of grating line density and orientation is feasible. In Fig. 7 b) the distance “a” corresponds to a shift up to a (phase) mismatch of 0.5 grating lines whereas “b” indicates the mismatch of a whole period of the grating. The center detection of the zero-Moiré-region can be supported by suitable fit functions in an evaluation step. Thus a sub-pixel accuracy can be achieved and this in turn corresponds to a very small fraction of the grating period (or wave length under measuring conditions). By this method we get a sensitivity comparable to a conventional interferometer only by detecting the centers of the best matching areas. Unlike to the interferometer measurement this approach needs a final evaluation step to retrieve the wave aberration from a set of discrete sampling points. However, despite the necessity of graphic rectification of the captured images due to the variation of projection conditions caused by moved/rotated optical components in the setup, it is based on today’s typical computer performance a comparable fast and easy way.

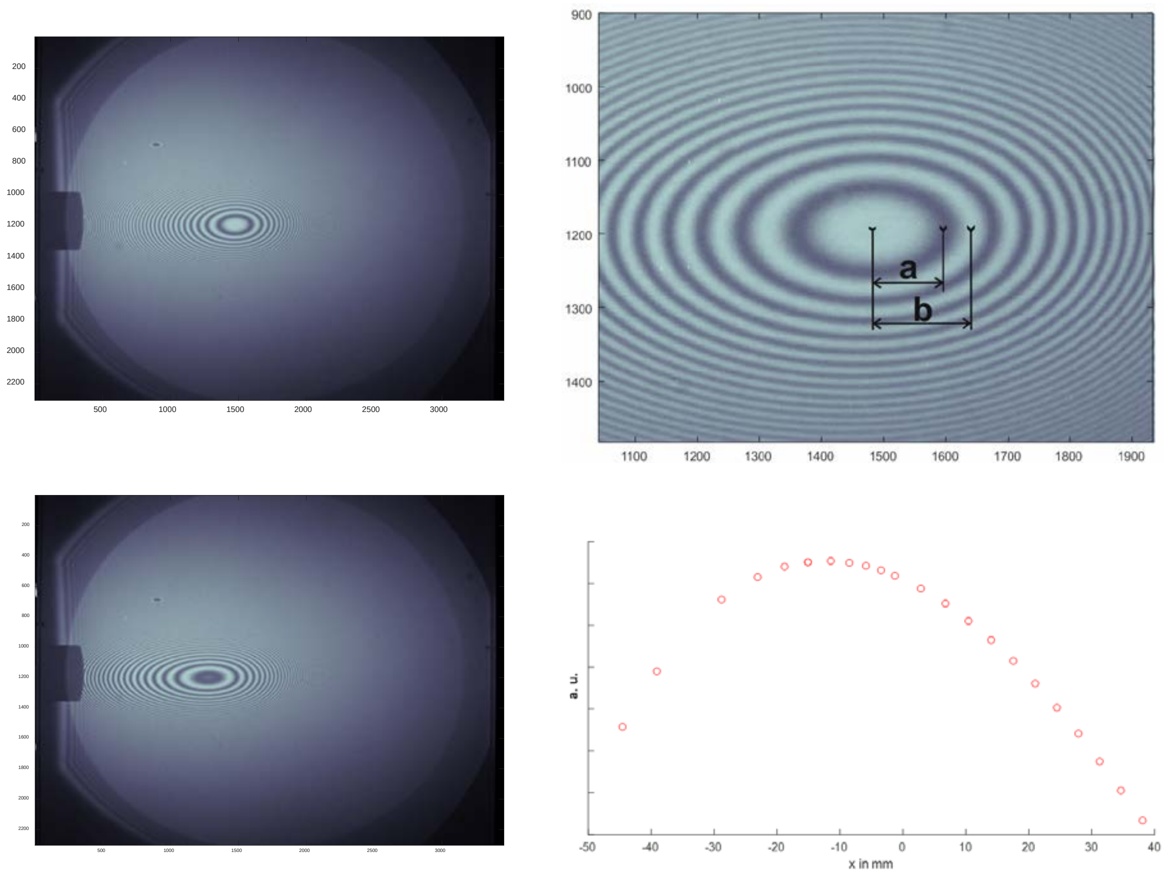

Fig. 7: a) Moiré-pattern of the whole clear aperture of the VLS grating (circular, diameter 100 mm);
b) Magnified region centered to the best matching area between test field and local grating line density with indication of meaning;
c) Moiré-pattern with grating rotation of 0.1000 degrees in relation to Fig. 5 a)
d) Derived line density distribution – the variation on the sample grating is about 0.5%

4. SUMMARY

The present paper reports about two different approaches of holographic setups – to create symmetrical and blazed resist profiles - and their adaption for the generation of tailored grating structures even on curved substrates. The prerequisite of an adapted measurement technique to complete the holographic process chain is a central statement. Our new approach in its basic configuration is able to identify the wave front aberration of a classical Offner type grating. An additional option for an adaption of the interference field to locally varying line densities enables the investigation of VLS gratings as well. The measurement technique works virtually independent of the substrate shape and its accuracy is in the range of lambda/20 using the existing test setup. The methods became a standard measurement technique developed at ZEISS during the past years. They can be used for the prediction and analysis of the spectrometer performance employing the investigated gratings.

5. ACKNOWLEDGEMENTS

The authors thank Matthias Burkhardt for the first results and the introduction of the newly developed method of the wave front measurements on Offner-type and VLS-gratings.

6. REFERENCES

[1] M. Heusinger, M. Banasch, U.D. Zeitner "Rowland ghost suppression in high efficiency spectrometer gratings fabricated by e-beam lithography," Opt. Express 25 (6), 6182-6190 (2017).
[2] P. Triebel, T. Diehl et al." Optical gratings and grisms: Developments on straylight and polarization sensitivity improved microstructures", Proceedings of SPIE Vol. 9611, 9611-44, 2015
[3] Alexandre Gatto, "Microstructured optics for high performance optical systems", Proceedings of SPIE Vol. 8613, 86130U (2013)
[4] Oliver Sandfuchs, Matthias Burkhardt, Reinhard Steiner, Alexandre Gatto, Robert Brunner, " Holographically microstructured gratings for high-performance spectrometers", DGaO Proceedings 2011, http://www.dgaoproceedings. de, ISSN: 1614-8436, 0287-2011-B027-2
[5] Pettinato, E. Fossati, P. M. Coppo, A. Taiti, D. Labate, A. Capanni, L. Erdmann, P. Triebel, M. Taccola, J. L. Bézy, M. Francois, R. Meynart, L. Erdmann, P. Triebel, "Instrument pre-development activities for FLEX", Proceedings Volume 10423, Sensors, Systems, and Next-Generation Satellites XXI; 1042305 (2017)
[6] Peter Triebel; Torsten Diehl; Tobias Moeller; Alexandre Gatto; Alexander Pesch; Lars H. Erdmann; Matthias Burkhardt; Alexander Kalies, "Enhanced monolithic diffraction gratings with high efficiency and reduced polarization sensitivity for remote sensing applications", Proceedings Volume 9641, Optics in Atmospheric Propagation and Adaptive Systems XVIII
[7] http://www.tropomi.eu
[8] https://sentinels.copernicus.eu/web/sentinel/missions/sentinel-5p
[9] Reinhard Steiner, Alexander Pesch, Lars H. Erdmann, Matthias Burkhardt; Alexandre Gatto, Robert Wipf, Torsten Diehl, H. J. P. Vink, B. G. van den Bosch "Fabrication of low stray light holographic gratings for space applications", Proc. of SPIE Vol. 8870 (2013)
[10] Fleming, Madeleine B.; Hutley, M. C., Blazed diffractive optics, 1997, Applied Optics 36(20) 4635-4643
[11] Hutley, M. C.; Hunter, W. R., Variation of blaze of concave diffraction gratings, 1981, Applied Optics, 20(2) 245-250